

Stochastic sparse adversarial attacks

Hatem Hajri¹, Manon Césaire^{1,3}, Théo Combey², Sylvain Lamprier³,

Patrick Gallinari^{3,4}

¹ IRT SystemX, 8 Avenue de la Vauve, 91120 Palaiseau, France
 hatem.hajri, manon.cesaire@irt-systemx.fr

² CentraleSupélec, 3 Rue Joliot-Curie 91192, Gif-sur-Yvette, France
 theo.combey@student-cs.fr

³ Sorbonne Université, CNRS, LIP6, F-75005 Paris, France

⁴ Criteo AI Lab, Paris, France
 sylvain.lamprier, patrick.gallinari@lip6.fr

Abstract. Adversarial attacks of neural network classifiers (NNC) and the use of random noises in these methods have stimulated a large number of works in recent years. However, despite all the previous investigations, existing approaches that rely on random noises to fool NNC have fallen far short of the-state-of-the-art adversarial methods performances. In this paper, we fill this gap by introducing stochastic sparse adversarial attacks (SSAA), standing as simple, fast and purely noise-based targeted and untargeted attacks of NNC. SSAA offer new examples of sparse (or L_0) attacks for which only few methods have been proposed previously. These attacks are devised by exploiting a small-time expansion idea widely used for Markov processes. Experiments on small and large datasets (CIFAR-10 and ImageNet) illustrate several advantages of SSAA in comparison with the-state-of-the-art methods. For instance, in the untargeted case, our method called voting folded Gaussian attack (VFGA) scales efficiently to ImageNet and achieves a significantly lower L_0 score than SparseFool (up to $\frac{1}{14}$ lower) while being faster. In the targeted setting, VFGA achieves appealing results on ImageNet and is significantly much faster than Carlini-Wagner L_0 attack.

1 Introduction

Adversarial machine learning has been essential in improving robustness of neural networks in recent years. Most of the work in this field has been centered around three categories of attacks according to the minimised distance between original and adversarial samples: L_2 (squared error) [19,12,3], L_∞ (max-norm) [6,10,9] and much less L_0 (or sparse) attacks (minimising the number of modified components). For L_0 attacks, a list of the most influential works, also related to our paper might be given [3,14,17,11,2,13,1,5].

Given a NNC $F : \mathbb{R}^n \rightarrow \mathbb{R}^p$, the predicted label for an input x is $\text{label}(x) = \underset{k}{\text{argmax}} F_k(x)$, where F_1, \dots, F_p are the class probabilities of F . We recall that

an adversarial example to x is an item x^* such that $\text{label}(x^*) \neq \text{label}(x)$ (un-targeted attack), or such that $\text{label}(x^*) = c$, with $c \neq \text{label}(x)$ a specific class (targeted attack).

Sparse alterations can be encountered in many situations and have been motivated in the previous works. For instance, they could correspond to some rain-drops on traffic signs that are sufficient to fool an autonomous driver [11]. Understanding these special perturbations is fundamental to mitigate their effects and take a step forward trusting neural networks in real-life.

This paper presents a general probabilistic approach to generate new L_0 attacks which rely on random noises. We argue that existing deterministic attacks, which classically perform by sequentially applying maximal perturbations on selected components of the input, fail at reaching accurate adversarial examples on real-world large scale datasets.

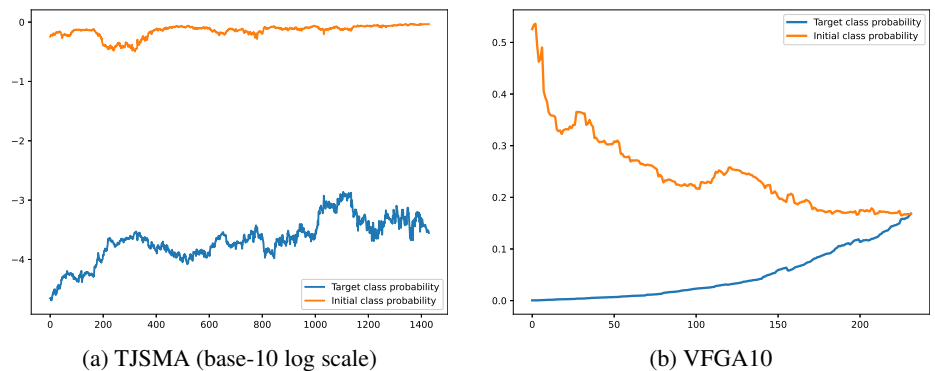


Fig. 1: Plots of the initial and targeted class probabilities for TJSMA on the left failing to converge along more than 1400 iterations and our VFGA10 method converging efficiently in less than 250 iterations on the right.

Figure 1 (left) illustrates this failure on the ImageNet dataset [15] for the one-component version of a state-of-the-art approach, named TJSMA [5], which does not succeed to affect the initial probability of the input on the Inception-v3 network [18]. On the other hand, working with more than one component at a time, while more accurate, does not scale at all on datasets as ImageNet. An alternative would be to repeatedly apply very small perturbations on components, but this would be at a high cost of efficiency. Our claim is that random attacks, while not much studied in the literature of L_0 adversarial attacks, are able to cope with these issues.

Stochastic sparse adversarial attacks (SSAA) are inspired by the study of stochastic diffusions, their infinitesimal generators and boundary behaviors. They follow main existing L_0 attacks, which rely on iteratively selecting the most salient input feature by means of saliency maps, but consider probabilistic distributions for component and intensity selections. After identifying the best component to alterate first, the process samples intensities of perturbations for the selected component and chooses the best move among them. This allows to obtain accurate adversarial samples more efficiently than approaches based on deterministic perturbations. Experimental results on large scale datasets, as depicted on the same example as the failure case of TJSMA in Figure 1 (on the right), show that our SSAA approaches (denoted VFGA10) succeed at efficiently producing accurate attacks in most cases.

The rest of the paper is organised as follows. Section 2 posits our contribution w.r.t related works. Section 3 introduces our SSAA. In Sections 4 and 5, we experiment SSAA on deep NNC on CIFAR-10 [8] and ImageNet [15] and compare their performances with the-state-of-the-art methods. Section 6 presents a conclusion and possible continuations of this work.

2 Related Work

In this section, we review related works on sparse attacks and outline our main contributions. We assume that inputs to the NNC F are in $[0, 1]^n$ and call Z_1, \dots, Z_p the output logits of F . Moreover, we fix c a targeted class label.

SparseFool [11]. This method is untargeted and geometric iterative. At each iteration, it applies DeepFool [12] to estimate the minimal adversarial perturbation thanks to a linearization of a classifier. Then, it estimates the boundary point and the normal vector of the decision boundary and updates the input features with a linear solver. To further improve this attack, [11] introduces a parameter λ to control the trade-off between the success rate, the number of perturbed input features and the complexity of the attack. Up to our knowledge, SparseFool is the fastest among all efficient untargeted attacks on ImageNet.

XSMA (JSMA [14], WJSMA, TJSMA [5]). These methods add deterministic maximal perturbations to the most salient input features which are selected by Jacobian-based saliency maps. The “one-pixel” variant of these maps roughly chooses the input feature with the highest $\frac{\partial Z_c}{\partial x_i}$ and lowest $\sum_{j \neq c} p_j \frac{\partial Z_c}{\partial x_i}$ score,

where $p_j = 1$, $p_j = F_j$ and $p_j = F_j(1 - x_j)$ respectively for JSMA, WJSMA and TJSMA. The “two-pixels” versions of these approaches select best pairs of components to perturb at each iteration, following the same principle as their

“one-pixel” counterpart. They have more ability to find salient input features and yield more successful attacks. Despite their effectiveness and speed advantage on low dimensional datasets, the major drawback of the XSMA is that they are not scalable to high dimensional data in their “two-pixels” versions, because of the high cost induced to compute saliency maps for pairs of features [3], and the “one-pixel” variants usually fail to converge as illustrated above in Figure 1. We claim that an important source of instability of these methods comes from the fact that once features to perturb are identified, maximal perturbations are applied to them. Due to the complexity of NNC on large scale data, Jacobians may be very unstable. Thus, applying such predefined deterministic perturbations can lead to destructive moves for the targeted probability. An alternative could be to only apply small - near infinitesimal - perturbations at each step of the process, but this would be at the cost of a very high complexity. To overcome this issue, the proposal of SSAA is to generate several random perturbations from a certain distribution discussed later, to allow more flexibility, and choose the best move after exploration of different intensities.

Carlini-Wagner L_0 attack (CW) [3]. This attack is obtained by solving the optimisation problem:

$$\text{Minimise } \|r\|_0 + cf(x+r), \quad s.t. \ x+r \in [0,1]^n \quad (1)$$

where $\|r\|_0$ is the L_0 distance of the perturbation r added to x and $f(x) = \left(\max_{i \neq c} Z_i(x) - Z_c(x) \right)^+$. Given the difficulty to deal with the L_0 norm in optimisation, the authors of [3] solve (1) relying on their L_2 attack and an algorithm that iteratively discards the components with no much effect on the output classification. Despite its high efficiency, CW is computationally expensive and much slower than the XSMA (for instance, it is found 20 times slower than JSMA in [3] and 50 times slower than TJSMA in [5]). This attack also requires hyperparameter tuning and pre-testing over data.

Gaussian attacks. In [2], the authors formulate the problem of adversarial attacks by the Gaussian noise $\mathcal{N}(\mu, \sigma^2 I_n)$ as follows:

$$\operatorname{argmin}_{\mu, \sigma} \left(\max_{i \neq c} \mathcal{E}_i(\mu, \sigma^2) - \mathcal{E}_c(\mu, \sigma^2) \right) \quad (2)$$

where $\mathcal{E}_i(\mu, \sigma^2) = \mathbb{E}[Z_i(x + \sigma^2 I_n)]$. Adversarial examples are then generated by sampling perturbations from $\mathcal{N}(\mu_0, \sigma_0^2 I_n)$ whose μ_0 and σ_0^2 are the optimal solutions to (2). Recently, [1] adapts this method by adding constraints on the maximum distortion of μ and constructs sparse and smooth Gaussian attacks that are perceptually feasible. Despite this progress on the use of random noise

in adversarial attacks, the general approach of [2,1] does not reach the-state-of-the art results. Secondly, it is restricted to NNC with ReLU activations. In contrast, SSAA achieve state-of-the art results on L_0 adversarial attacks while being much less complex in comparison with [2,1] and also applicable on general NNC.

3 Stochastic sparse Attacks

In this section, we introduce our stochastic sparse attacks, by means of Gaussian noises on selected components of the input. To simplify the presentation, we mainly discuss targeted attacks and then deduce untargeted ones by applying slight modifications. The aim herein is to iteratively identify the best component to perturb and the best move for this component until the target label becomes the most probable for the NNC.

Consider a Gaussian noise $X_\theta \sim \mathcal{N}(0, \theta)$ and denote by (e_1, \dots, e_n) the basis of \mathbb{R}^n . Any c -targeted probability expectation of the perturbed input $x + X_\theta e_i$ can be expanded as follows:

$$\mathbb{E}[F_c(x + X_\theta e_i)] = F_c(x) + \theta(\mathcal{G}_i F_c)(x) + \dots \quad (3)$$

where $\mathcal{G}_i F_c = \frac{1}{2} \frac{\partial^2 F_c}{\partial^2 x_i}$ is the infinitesimal generator of X_θ seen as a diffusion. When taking the folded Gaussian noise $X_\theta \sim |\mathcal{N}(0, \theta)|$, this expansion becomes:

$$\mathbb{E}[F_c(x + X_\theta e_i)] = F_c(x) + \sqrt{\frac{2\theta}{\pi}} \frac{\partial F_c}{\partial x_i} + \theta(\mathcal{G}_i F_c)(x) + \dots \quad (4)$$

We build our reasoning upon a heuristic which is to look for the input feature i that maximizes $\mathbb{E}[F_c(x + X_\theta e_i)]$. The assumption behind this heuristic is that searching for the best expectation will allow to discover the best moves according to the distribution of the noise X_θ . This does not hold for the Gaussian noise $X_\theta \sim \mathcal{N}(0, \theta)$, since in that case the approximations $\mathbb{E}[F_c(x + X_\theta e_i)] \approx F_c(x) + \theta(\mathcal{G}_i F_c)(x)$ and $Var[F_c(x + X_\theta e_i)] \approx \theta(\frac{\partial F_c}{\partial x_i})^2$ are of the same order of θ , indicating that variance should be taken into account in selecting best components to perturb. On the other hand, considering the folded Gaussian noise $|X_\theta|$ and using the approximation $\mathbb{E}[F_c(x + X_\theta e_i)] \approx F_c(x) + \sqrt{\frac{2\theta}{\pi}} \frac{\partial F_c}{\partial x_i}$ induces a negligible variance (only terms of θ^p with $p \geq 1$) in front of the expectation, at least when $|\theta| < 1$. This means that working with the folded Gaussian distribution allows us to only focus on the expected probability of the perturbed input. Note also that the approximation of this expected probability only contains first

derivatives w.r.t. to the input component which is a practical advantage of the folded over the pure Gaussian noise.

While it would have been possible to consider some combination of $\mathbb{E}[F_c(x + X_\theta e_i)]$ and $Var[F_c(x + X_\theta e_i)]$ for the Gaussian noise, taking a folded noise presents an important additional advantage for bounded inputs. Please note that, without loss of generality, we consider inputs bounded in $[0, 1]$ in this paper, as well as the adversarial samples which share the same support domain. In the following, we propose to automatically tune the variance parameter θ of X_θ according to the distance of the input x_i to these bounds. Please note that, for a given component i , $x_i \neq 0.5$, the possible amplitude of move is not the same in both directions. Considering a Gaussian noise, since symmetric, would be problematic for this θ tuning. Rather, considering two folded Gaussian noises for each component, one positive (only for component increase) and one negative (only for component decrease) allows better fitted selections.

In the following, we first present a one-sided, only increasing perturbations, stochastic attack based on folded Gaussian noises. Then, we deduce a both-sides attack, that considers the best choice between increase and decrease of each component, called Voting Folded Gaussian Attack.

3.1 Folded Gaussian Attack (FGA)

For our one-side targeted attack FGA, the most relevant input feature to perturb is thus selected by the rule $i_0 = \underset{i}{\operatorname{argmax}} \sqrt{\theta_i} \frac{\partial F_c}{\partial x_i}$, considering a folded Gaussian noise $|\mathcal{N}(0, \theta_i)|$.

Choosing the variance θ_i . Since FGA only considers positive perturbations of the input, fixing the variance θ_i must consider the upper-bound of the input domain. A quite natural choice could be either $\theta_i = 1 - x_i$ (variance = $1 - x_i$) or $\sqrt{\theta_i} = (1 - x_i)$ (standard deviation = $1 - x_i$). Our recommendation, which we follows, is to choose $\theta_i = 1 - x_i$. We do not possess a theoretical justification of this choice. First, it is fixed while keeping the famous analogy time = variance in the study of diffusions. Since the XSMA add a “time” $1 - x_i$, we fixed our variance in the same way which also gives us better performance results than the second alternative.

After selecting the input feature i , our proposal is to simulate N_S samples from $|\mathcal{N}(0, \theta_i)|$ to find an accurate move towards a close adversarial sample. The complete process is depicted in Algorithm 1, which introduces the increasing FGA (and the decreasing FGA by analogy).

Choosing N_S . The number N_S is the main hyper-parameter of Algorithm 1. From its definition, one can expect that increasing N_S will increase, up to sat-

Algorithm 1 (Increasing) Folded Gaussian Attack (FGA)

Inputs x : input of label l , $c \neq l$: targeted class
 N_S : number of samples to generate
maxIter: maximum number of iterations
Output \tilde{x} : adversarial sample to x .

1: Initialise: $\tilde{x} = x$, **Iter** = 0, $\Gamma = \{1, \dots, \dim(x)\} \setminus \{i : x_i = 1\}$.

2: **While** $\Gamma \neq \emptyset$, $\text{label}(\tilde{x}) \neq c$ and **Iter** < **maxIter** **do**

3: $i_0 = \underset{i \in \Gamma}{\text{argmax}} \sqrt{1 - x_i} \frac{\partial F_c}{\partial x_i}(x)$.

4: Generate samples $(S^h)_{1 \leq h \leq N_S}$ from $|\mathcal{N}(0, \theta)|$ where $\theta := (1 - x_i)$.

5: For $h \in [1 : N_S]$, define the input \tilde{y}^h by

$$\tilde{y}_{i_0}^h \leftarrow \text{Clip}^\theta \left(\tilde{x}_{i_0} + S^h \right) \text{ and } \tilde{y}^h = \tilde{x} \text{ on the rest of the components}$$

6: Batch compute $F_c(\tilde{y}^h, h \in [1 : N_S])$

7: Update $\tilde{x} = \underset{\tilde{y}^h}{\text{argmax}} F_c(\tilde{y}^h)$

8: $\Gamma = \Gamma \setminus \{i_0\}$, **Iter** ++

9: **return** \tilde{x}

uration, the effectiveness of the attacks. This may, however, slow down their speeds. Thanks to batch computing in Step 7, with sufficient memory, Step 6 can be performed at the cost of $N_S = 1$ and (reasonably) augmenting N_S makes Algorithm 1 converge faster as less iterations are needed. In all our experiments, we fix this number to $N_S = 10$. We remark that the obtained attacks are more efficient than those with $N_S = 1$ but not very different from those with $N_S = 20$ which are slower. Finally, we also notice that batch computing used here does not often require a parallel computing effort by the attacker as this option is available in standard libraries.

While the previous process only applies perturbations that increase the input, lowering the input features intensities can be as effective as increasing them. Following the same analogy, we introduce the decreasing FGA attack by taking $\theta_i = x_i$ rather than $\theta_i = (1 - x_i)$ and replacing $|\mathcal{N}(0, \theta)|$ with $-|\mathcal{N}(0, \theta)|$ in the previous algorithm.

Note that FGA and XSMA are one sided attacks but, while XSMA apply predefined maximal perturbations, FGA explores in real time best perturbations to apply.

3.2 Voting Folded Gaussian Attack (VFGA)

In this section, we propose a two-sided attack, which both considers $\mathbb{E}[F_c(x + |X_{\theta_i^+}|e_i)]$ and $\mathbb{E}[F_c(x - |X_{\theta_i^-}|e_i)]$ for each feature, with $X_\theta \sim \mathcal{N}(0, \theta)$, $\theta_i^+ = (1 - x_i)$ and $\theta_i^- = x_i$. This method applies increasing and decreasing FGA at each iteration and chooses the most effective moves in both directions. Details are given in Algorithm 2.

Algorithm 2 Voting Folded Gaussian Attack (VFGA)

Same inputs and outputs as Algorithm 1

- 1: Initialise: $\tilde{x} = x$, $\text{Iter} = 0$, $\Gamma = \{1, \dots, \dim(x)\}$
 - 2: **While** $\Gamma \neq \emptyset$, $\text{label}(\tilde{x}) \neq c$ and $\text{Iter} < \text{maxIter}$ **do**
 - 3: $i^+ = \underset{i \in \Gamma}{\operatorname{argmax}} \sqrt{1 - x_i} \frac{\partial F_c}{\partial x_i}(x)$
 - 4: $i^- = \underset{i \in \Gamma}{\operatorname{argmin}} \sqrt{x_i} \frac{\partial F_c}{\partial x_i}(x)$.
 - 5: Generate samples $(S^{+,h})_{1 \leq h \leq N_S}$ from $|\mathcal{N}(0, \theta_i^+)|$ where $\theta_i^+ := (1 - x_{i^+})$
 - 6: Generate samples $(S^{-,h})_{1 \leq h \leq N_S}$ from $-\mathcal{N}(0, \theta_i^-)$ where $\theta_i^- := x_{i^-}$
 - 7: For $h \in [1 : N_S]$, define the inputs \tilde{y}^\pm by
 - 8: $\tilde{y}_{i^\pm}^{\pm,h} \leftarrow \operatorname{Clip}(\tilde{x}_{i^\pm} + S^{\pm,h})$ and $\tilde{y}^{\pm,h} = \tilde{x}$ on the rest of the components.
 - 9: Batch compute $F_c(\tilde{y}^{\pm,h}, h \in [1 : N_S])$
 - 10: Update $\tilde{x} = \underset{\tilde{y}^{\pm,h}}{\operatorname{argmax}} F_c(\tilde{y}^{\pm,h})$
 - 11: $\Gamma = \Gamma \setminus \{i_0\}$, with $i_0 \in \{i^+, i^-\}$ (according to Step 13)
 - 12: $\text{Iter} ++$
 - 13: **return** \tilde{x} .
-

3.3 Untargeted SSAA

The main focus for these attacks is to decrease the class probability of the input until a new class label is found. Few modifications are required to deduce the untargeted versions of the previous Algorithms: by assuming c is the true label of x and replacing the argmax with argmin in Steps 3 and 7 of Algorithm 1.

4 Experiments on untargeted attacks

In this section, we conduct experiments on various network architectures and datasets to highlight the benefits of untargeted SSAA. Our attacks FGA and VFGA, with the sampling number $N_S = 10$, therefore called **FGA10** and **VFGA10** are challenged and compared against the SparseFool state-of-the-art method. Two datasets illustrating small and high dimensional data are considered: CIFAR-10 [8] and ImageNet [15]. We recall that CIFAR-10 contains $32 \times 32 \times 3$ color images divided into 10 different classes. For ImageNet, we consider the ILSVRC2012 dataset containing approximately 1.2 million color images of size $299 \times 299 \times 3$ divided into 1,000 classes. The experiments carried out on each dataset, including the used network models, are described and analysed in the upcoming paragraphs. We notice that SparseFool attacks were generated relying on the original Pytorch implementation of this method after fixing the control parameter λ to $\lambda = 3$ as recommended in [11]. For the sake of comparison, our attacks in this section are also implemented with Pytorch. All experiments in the present and next section are carried out on GPU ⁵.

To assess the attacks performances, we compute the success rate (SR) defined as the percentage of the successfully crafted samples, without restriction on `maxIter`. Second, we report the average L_0, L_1, L_2 distances between inputs and the corresponding adversarial samples simply denoted L_i . Also, we report the best and worst L_0 distances and finally measure the average-time (in second) to generate an adversarial sample.

4.1 On CIFAR-10.

The architectures used on this dataset are ResNet18 [7] and VGG-19 [16]. After training these two models with Pytorch, we obtained the performances given in Table 1.

Models	Accuracy in Train	Accuracy in Test
ResNet18	98.39 %	90.91 %
VGG-19	97.99 %	89.76 %

Table 1: Accuracies of the Pytorch CIFAR-10 models.

In addition to FGA10, VFGA10, SparseFool, we also test the following method as a baseline on CIFAR-10:

⁵ NVIDIA Tesla P100 (16Go) GPU.

Uniform attack (UA). This method adds random uniform noises instead of folded Gaussian ones. It follows the lines of Algorithm 1 (in its untargeted form), but Step 3 is replaced with $i_0 = \underset{i \in \Gamma}{\operatorname{argmin}} (1 - x_i) \frac{\partial F_c}{\partial x_i}(x)$ and sampling in Step 4 is done from $\mathcal{U}([0, \theta_i])$, $\theta_i = 1 - x_i$. We consider the variant UA10 corresponding to the sampling number $N_S = 10$.

In Table 2, we report the performances of all the attacks on the well predicted samples among the 10,000 test images of CIFAR-10.

Attacks	SR	L_0	L_1	L_2	Best L_0	Worst L_0	Time (sec.)
ResNet18							
SparseFool	100	30.78	73.34	10.59	1	477	0.688
UA10	100	8.19	12.07	4.26	1	76	0.679
FGA10	100	5.58	7.52	3.36	1	54	0.452
VFGA10	100	4.13	7.25	3.76	1	39	0.429
VGG-19							
SparseFool	100	26.23	41.79	8.62	1	1032	0.621
UA10	100	6.86	9.88	3.86	1	99	0.832
FGA10	100	5.79	6.69	3.07	1	98	0.788
VFGA10	100	3.43	5.43	3.14	1	59	0.612

Table 2: Results on the well predicted among the 10,000 test images of CIFAR-10. L_i refers to the average L_i and Time is the average-time to generate one sample.

Although all attacks attain 100% SR, it is obvious that ours largely exceed SparseFool regarding all metrics. For both models, FGA10 and VFGA10 alterate up to 5 and 7 times fewer features comparing with SparseFool. The remarkable advantage of FGA10 and VFGA10 relative to the worst L_0 score also demonstrates that our attacks are much more stable. We also notice that VFGA10 is the most efficient attack on the two models which showcases the interest of combining positive and negative folded Gaussian distributions. On ResNet18, this attack modifies in average 0.134% of the input features, while this is near 0, 112% on VGG-19. On the other hand, despite the equality for the SR and best L_0 , FGA10 has overall better scores than UA10. This highlights the relevance of the folded Gaussian noise over the uniform one. Comparing the attacks speed, VFGA10 is up to 1.6 times faster than SparseFool and UA10 on the ResNet18 model and obtains slightly better speed results on the VGG-19 model. FGA10 is also faster than UA10.

Augmenting N_S . In what follows, we investigate the impact of augmenting N_S on the performances of our attacks by testing FGA20 and VFGA20 which are FGA and VFGA with $N_S = 20$ on the same data as Table 2. Also, as a further comparison, we evaluated the performances of UA20, which is the UA with $N_S = 20$. Table 3 reports the results of each attack.

Attacks	SR	L_0	L_1	L_2	Best L_0	Worst L_0	Time (sec.)
ResNet18							
UA20	100	7.79	10.34	3.79	1	65	0.721
FGA20	100	5.48	7.31	3.32	1	31	0.606
VFGA20	100	4.13	7.12	3.72	1	44	0.578
VGG-19							
UA20	100	6.23	9.35	3.43	1	137	0.951
FGA20	100	5.66	6.22	2.97	1	132	0.913
VFGA20	100	3.40	5.31	3.10	1	53	0.808

Table 3: Similar results to Table 2 with $N_S = 20$.

First, we notice that FGA20 and VFGA20 achieve slightly better, but not very meaningful, L_i scores. Based on the speeds evaluation, they are however significantly slower than FGA10 and VFGA10. This illustrates that increasing so much N_S may not significantly improve but on the other hand it may slow down the attacks. Second, we observe that despite augmenting N_S from 10 to 20, the uniform attack can not beat FGA10. This is quite remarkable since for the uniform distribution the N_S generated samples are almost surely different and inside the domain of the input features while for the folded Gaussian distribution, due to clipping, several samples are likely to be clipped at the maximal value.

4.2 On ImageNet.

In this section, we re-test our FGA10 and VFGA10, defined in the previous section and compare them against SparseFool on ImageNet. Two pre-trained models provided by PyTorch are considered for testing: Inception-v3 [18] and VGG-16 [16] whose accuracies are respectively 77.45% and 71.59%. We have chosen to challenge the three attacks on the firstly 7,500 well predicted ImageNet test images. Table 4 displays the results obtained after experimentations.

Attacks	SR	L_0	L_1	L_2	Best L_0	Worst L_0	Time (sec.)
Inception-v3							
SparseFool	100	480.92	782.13	31.67	1	4100	48.47
FGA10	100	237.27	238.14	17.75	1	4856	31.46
VFGA10	100	53.08	42.10	7.06	1	4153	7.14
VGG-16							
SparseFool	100	362.31	776.54	42.49	1	3318	34.32
FGA10	100	181.10	197.48	18.58	1	4599	23.87
VFGA10	100	25.21	25.36	6.05	1	1932	3.26

Table 4: Results on the firstly 7, 500 well predicted test images of ImageNet. L_i refer to the average L_i and Time is the average-time to generate one sample.

First, we notice the same maximal SR for all the attacks but as for the CIFAR-10 experiments, FGA10 and VFGA10 largely outperform SparseFool for all the average distances. In particular, FGA10 modifies more than half as many features as SparseFool. Moreover, VFGA10 changes more than 9 times (resp. 14 times) fewer features than SparseFool on Inception-v3 (resp. VGG-16). On Inception-v3, VFGA10 alters in average 0.0198% of the input features and the results are even better with the VGG-16 model since VFGA10 modifies in average 0,00940% of the features. Although all attacks reach the best possible L_0 score, our experiments demonstrate that many samples were crafted within one iteration much more with our attacks than SparseFool. Indeed, the best score $L_0 = 1$ was reached by SparseFool, FGA10 and VFGA10 on Inception-v3 for near 0.346% – 0.653% – 1.2% of the samples. On VGG-16, these values are as follows: 0.467% – 1.12% – 2.4%. As an illustration, Figure 2 shows an example of this one iteration success for VFGA10 on Inception-v3.

The only slight advantage of SparseFool that can be pointed out from the previous table is that it beats FGA10 and slightly beats VFGA10 for the worst L_0 score on Inception-v3. As a second illustration, Figure 3 shows the original and adversarial image obtaining the worst L_0 for VFGA10. Visually, one recognizes the same class label as the original input despite it has the worst L_0 score.



(a) Weimaraner (proba.=0.3775)



(b) Burrito (proba.=0.1399)

Fig. 2: One of the best untargeted performances on Inception-v3: $L_0 = 1$ (the modified pixel can be observed on the adversarial sample). The probability of Weimaraner passes to 0.0447 after one iteration.



(a) Zebra (proba.=0.9397)



(b) Tub (proba.=0.0279)

Fig. 3: Worst untargeted performance on Inception-v3 : $L_0 = 4153$.

Finally, results on speed, demonstrate that our attacks are significantly faster than SparseFool. In particular, for both models, VFGA10 is about 7 to 10 time faster than SparseFool.

5 Experiments on targeted attacks

This section presents experiments on targeted SSAA and provides comparison with some state-of-the-art and baselines targeted L_0 attacks on the same two datasets as the previous section. Again, we challenge our attacks FGA10 and VFGA10 which correspond to targeted FGA and VFGA with $N_S = 10$. For the sake of comparison with the-state-of-the-art, our attacks in this section are implemented with TensorFlow.

5.1 On CIFAR-10.

In what follows, we compare our methods against TJSMA (in its two-pixels form) and CW, which we discussed in Section 2. On CIFAR-10, we consider the same NNC as [5] with accuracy 83.81 % and limit the maximum number of modifiable pixels to `maxIter` = 114 for all the attacks as [5]. This allows to generate or use the results of TJSMA and CW from [5]. In addition to TJSMA and CW, we introduce and test the following baseline:

Gaussian attack (GA). This method applies the Gaussian noise and is derived starting from the expansion 3. It follows Algorithm 1 by replacing Step 3 with $i_0 = \underset{i \in \Gamma}{\operatorname{argmax}}(1 - x_i) \frac{\partial^2 F_c}{\partial^2 x_i}(x)$ and sampling N_S times from $\mathcal{N}(0, \theta)$ in Step 4. We consider the variant GA10 which corresponds to $N_S = 10$. Note that we have made a choice to test increasing versions.

In our experiments, we tested FGA10, VFGA10, TJSMA and GA10 on the 1,000 firstly correctly-predicted CIFAR-10 test images. TJSMA was run using the original implementation of [5]. We did not run CW attack but rather reported its performances on the first 100 well-predicted test images, that is on 1,000 samples from [5]. Tables 5 and 6 display the performances of the four attacks.

Attacks	SR	L_0	L_1	L_2
FGA10	95.96	32.11	11.49	2.33
VFGA10	98.92	25.04	10.26	2.26
TJSMA	97.08	37.45	28.06	4.41
GA10	95.93	33.95	10.67	2.10

Table 5: Results on the 1,000 firstly correctly-predicted test images of CIFAR-10.

Attacks	SR	L_0
VFGA10	99.33	23.87
CW	99.89	24.97

Table 6: Results for VFGA10 and CW on the first 100 well predicted CIFAR-10 test images.

Comparison with TJSMA. It can be seen that FGA10 obtains slightly smaller SR but significantly better L_i scores than TJSMA. VFGA10 has a clear advantage over TJSMA according to all metrics, notably more than 12 pixels fewer in the L_0 score. The benefit of VFGA10 over FGA10 can also be noticed. A further privilege of VFGA over TJSMA is speed, mainly due to the significant L_0 advantage. This can be seen across Table 7 reporting the average time for TJSMA and VFGA10 to generate a successful adversarial sample. From that table, we notice that VFGA10 is near 2 times faster than TJSMA.

Attacks	TJSMA	VFGA10
Time (sec)	1.58 sec.	0.78 sec.

Table 7: Average time (in second) for generating an adversarial sample for TJSMA and VFGA10.

Comparison with GA10. FGA10 obtains slightly better SR and L_0 scores than this attack which is also very slow in comparison with both FGA and VFGA because of the high cost to compute second derivatives (more than 10 minutes to generate an adversarial image).

Comparison with CW. Relying on Table 6, VFGA has a slightly lower success rate but better L_0 score than CW. A more notable advantage of VFGA is that it is less complex and much faster than CW. As for a concrete speed comparison between these attacks on CIFAR-10, we believe that our comparison with TJSMA is quite sufficient to note our speed advantage over CW as the XSMA are known to be much faster than CW [3,5].

5.2 On ImageNet.

In this section, we challenge VFGA10 on two pre-trained ImageNet Keras models [4]: ResNet50 [7] and Inception-v3 [18] with accuracies 74.9% and 77.9%.

The inputs for both models are respectively of size $224 \times 224 \times 3$ and $299 \times 299 \times 3$. Since we are interested in targeted attacks and the number of ImageNet classes is too large, similarly to [3], we have made a simplification by selecting 100 targeted class labels which were generated randomly once for all before the experiments. Our method is then tested on the firstly 50 correctly-predicted ImageNet test images; which corresponds to 5,000 attacks (i.e., 50 images \times 100 targeted labels). We do not limit `maxIter` for the ResNet50 model, but limit it to `maxIter = 5000` for Inception-v3 as this model is more challenging. Again, we take CW as a baseline but given its high cost, we evaluate it only on the first 9 images; that is on 900 adversarial images using its original available code. Table 8 reports the SR and L_0 scores as defined in the previous section for both attacks.

Attacks	SR	L_0
ResNet50 model (no restriction on <code>maxIter</code>)		
VFGA10 on 5,000 samples	100	587.79
CW on 900 samples	100	378.76
Inception-v3 model (<code>maxIter = 5000</code>)		
VFGA10 on 5,000 samples	93.24	1455.66
CW on 900 samples	100	491.39

Table 8: Results obtained by VFGA10 and CW respectively on the 50 and 10 firstly correctly-predicted test images of ImageNet.

From Table 8, we note the high SR of VFGA10. Indeed, the attack reaches 100% SR on ResNet50 while modifying in average 0.39% of the input features. Our experiments show that the worst L_0 score in this case is 4828 pixels, corresponding to a maximum distortion of 3.2%. As for the Inception-v3 model, when successful, our attack modifies in average 0.54% of the input features. The worst obtained L_0 score in this case is 4978 pixels which corresponds to a maximum distortion of 1.8%. For both experiments, several samples were crafted within only one iteration.

Figure 4 and 5 show the images obtaining the best and worst performances by VFGA10 for the ResNet50 model on ImageNet with the benign image on the left and the adversarial one on the right. The respective class probabilities are put between parenthesis.



(a) Mousetrap (proba.=0.5572)



(b) Wood rabbit (proba.=0.5813)

Fig. 4: One of the best targeted performances on ResNet50: $L_0 = 1$. The probability of Mousetrap passes to 0.4066 after one iteration.



(a) Cab (proba.=0.9118)



(b) Turnstone (proba.=0.0681)

Fig. 5: Worst targeted performance on ResNet50: $L_0 = 4828$.

For the Inception-v3 model, VFGA10 modifies near $3 \times$ more input features than CW, while this is reduced to $2 \times$ more input features for the second model.

Of course our method does not beat the performance of CW. Despite this fact, it is able to reach a high level of efficiency. Second, it is much faster and

more practical than CW. Indeed, generating an adversarial sample by VGA10 took in average 3 minutes 38 seconds and 13 minutes 20 seconds per image on the ResNet50 and Inception-v3 models, respectively. The same task took several hours by CW on the same used machine.

6 Conclusion

This paper introduced noise-based attacks to generate sparse targeted and un-targeted adversarial samples from inputs to deep neural network classifiers. The proposed methods demonstrated high capabilities to generate adversarial examples and several advantages regarding the-state-of-the-art. Up to our knowledge, our paper is the first work to achieve such high performances using random noises. Our methodology relies on a simple expansion idea that provides a close link between adversarial machine learning and Markov processes. We believe it can be pursued in several ways. For instance, continuing with L_0 attacks, it seems important to understand the effects of noises that can be obtained as realisations of homogeneous Lévy processes with typical generators of the form

$$\mathcal{G}_i^{a,b} F_c(x) = a \frac{\partial F_c}{\partial x_i}(x) + \frac{b^2}{2} \frac{\partial^2 F_c}{\partial^2 x_i}(x) + \gamma \int (F_c(x + ye_i) - F_c(x)) \nu(dy)$$

where ν is a Lévy measure. Examples of such noises include the combination of deterministic, Gaussian and Poisson or compound Poisson noises which were not discussed in this paper. Even if approximating the jump (last) term would add some complexity to the approach, this problem sounds feasible and probabilistically attractive at least on small neural networks which are far from being completely understood. Among these methods, it seems interesting to derive those that can run fastly on large datasets by looking at their boundary behaviours as we did for the folded Gaussian method. Moreover, combining these attacks in a voting way can lead to very powerful L_0 attacks. Defence strategies have not been considered in this paper and may be very useful to make neural networks more robust.

Finally, even if we only discussed L_0 attacks throughout the paper, we believe that our approach can be extended to generate L_p adversarial attacks in general. This seems to us a very important question that comes out from our work.

References

1. Modar Alfadly, Adel Bibi, Emilio Botero, Salman Alsubaihi, and Bernard Ghanem. Network Moments: Extensions and Sparse-Smooth Attacks. *arXiv e-prints*, page arXiv:2006.11776, June 2020.

2. Adel Bibi, Modar Alfadly, and Bernard Ghanem. Analytic expressions for probabilistic moments of pl-dnn with gaussian input. In *The IEEE Conference on Computer Vision and Pattern Recognition (CVPR)*, June 2018.
3. N. Carlini and D. Wagner. Towards evaluating the robustness of neural networks. In *2017 IEEE Symposium on Security and Privacy (SP)*, pages 39–57, 2017.
4. François Chollet et al. Keras. <https://keras.io>, 2015.
5. Théo Combey, António Loison, Maxime Faucher, and Hatem Hajri. Probabilistic Jacobian-based Saliency Maps Attacks. *Mach. Learn. Knowl. Extr.* 2, no. 4, page 558.
6. I J Goodfellow, J Shlens, and C Szegedy. Explaining and harnessing adversarial examples. *ICLR*, 1412.6572v3, 2015.
7. Kaiming He, Xiangyu Zhang, Shaoqing Ren, and Jian Sun. Deep residual learning for image recognition. In *2016 IEEE Conference on Computer Vision and Pattern Recognition, CVPR 2016, Las Vegas, NV, USA, June 27-30, 2016*, pages 770–778. IEEE Computer Society, 2016.
8. Alex Krizhevsky, Vinod Nair, and Geoffrey Hinton. Cifar-10 (Canadian institute for advanced research).
9. A Kurabin, I J Goodfellow, and S Bengio. Adversarial examples in the physical world. *ICLR*, 1607.02533v4, 2017.
10. Aleksander Madry, Aleksandar Makelov, Ludwig Schmidt, Dimitris Tsipras, and Adrian Vladu. Towards deep learning models resistant to adversarial attacks. In *6th International Conference on Learning Representations, ICLR 2018, Vancouver, BC, Canada, April 30 - May 3, 2018, Conference Track Proceedings*. OpenReview.net, 2018.
11. Apostolos Modas, Seyed-Mohsen Moosavi-Dezfooli, and Pascal Frossard. Sparsefool: A few pixels make a big difference. In *IEEE Conference on Computer Vision and Pattern Recognition, CVPR 2019, Long Beach, CA, USA, June 16-20, 2019*, pages 9087–9096. Computer Vision Foundation / IEEE, 2019.
12. S. Moosavi-Dezfooli, A. Fawzi, and P. Frossard. Deepfool: A simple and accurate method to fool deep neural networks. In *2016 IEEE Conference on Computer Vision and Pattern Recognition (CVPR)*, pages 2574–2582, 2016.
13. Nina Narodytska and Shiva Prasad Kasiviswanathan. Simple Black-Box Adversarial Perturbations for Deep Networks. *arXiv e-prints*, page arXiv:1612.06299, December 2016.
14. N Papernot, P McDaniel, S Jha, M Fredrikson, Z Berkay Celik, , and A Swami. The limitations of deep learning in adversarial settings. *IEEE*, 1511.07528v1, 2015.
15. Olga Russakovsky, Jia Deng, Hao Su, Jonathan Krause, Sanjeev Satheesh, Sean Ma, Zhiheng Huang, Andrej Karpathy, Aditya Khosla, Michael Bernstein, Alexander C. Berg, and Li Fei-Fei. ImageNet Large Scale Visual Recognition Challenge. *International Journal of Computer Vision (IJCV)*, 115(3):211–252, 2015.
16. Karen Simonyan and Andrew Zisserman. Very deep convolutional networks for large-scale image recognition. In Yoshua Bengio and Yann LeCun, editors, *3rd International Conference on Learning Representations, ICLR 2015, San Diego, CA, USA, May 7-9, 2015, Conference Track Proceedings*, 2015.
17. J. Su, D. V. Vargas, and K. Sakurai. One pixel attack for fooling deep neural networks. *IEEE Transactions on Evolutionary Computation*, 23(5):828–841, 2019.
18. Christian Szegedy, Vincent Vanhoucke, Sergey Ioffe, Jonathon Shlens, and Zbigniew Wojna. Rethinking the inception architecture for computer vision. *CoRR*, abs/1512.00567, 2015.
19. Christian Szegedy, Wojciech Zaremba, Ilya Sutskever, Joan Bruna, Dumitru Erhan, Ian Goodfellow, and Rob Fergus. Intriguing properties of neural networks. In *International Conference on Learning Representations*, 2014.